

Infrared Combination Mode Absorption in Lithium-Boron-Doped Silicon

M. WALDNER AND M. A. HILLER

North American Aviation Science Center, Thousand Oaks, California

AND

W. G. SPITZER*

*Departments of Electrical Engineering and Materials Science, University of Southern California,
Los Angeles, California*

(Received 10 May 1965)

Infrared absorption bands due to double-quantum transitions of local lattice-mode vibrations in boron-lithium-doped silicon have been observed. The transitions are found near twice the frequency of all local modes and at the sum frequency of the two strongest local-mode vibrations, which are those associated with boron-lithium pairs. The relative strengths of the pair modes, the displacement of the modes from the mode due to isolated substitutional boron, and the relative strengths of the overtone absorption bands are consistent with the assumption of a predominantly Coulomb interaction between the boron and lithium ions. Five additional absorption bands, with frequency depending upon boron isotope, are found at frequencies not corresponding to sums of local-mode frequencies. Four of these bands occur at sum frequencies of the two strongest local-mode frequencies and of silicon critical-point phonon frequencies. The dependence of the frequency of all absorption peaks on lithium and boron isotopes is used to assist in the assignment of the absorption bands.

INTRODUCTION

PREVIOUS studies of boron-doped silicon electrically compensated with phosphorus¹ or antimony² or with neutron bombardment³ have confirmed the existence of infrared active local modes produced by the boron-10 or boron-11 substitutional impurities. The frequencies of the modes are close to those predicted by Dawber and Elliott.⁴ Similar local modes have been reported for substitutional carbon impurity in silicon.⁵ Introduction of lithium into boron-doped silicon to effect electrical compensation causes each of the boron bands to split into a high-frequency doubly degenerate band and a lower frequency nondegenerate band.⁶⁻⁸ In addition a new band is introduced at a frequency slightly greater than the highest silicon phonon frequency, the optical mode at the zone center. This local mode frequency is insensitive to boron mass and the mode has been found also in gallium-lithium- and aluminum-lithium-doped silicon.⁷

The above spectra may be interpreted qualitatively in terms of boron-lithium pair formation in the silicon

where the effective force constant between the boron and lithium is small compared to that between the boron and silicon. A study of the temperature dependence of the absorption at the central frequency and at the frequencies of the splitoff bands has confirmed the identification of the paired lithium ions as the perturbing element.⁷

In the present work we wish to report the observation of absorption bands in the boron-lithium-doped silicon at overtone frequencies of the local modes and at summation frequencies of the two strongest modes with silicon lattice phonons. Bands at overtones of local modes have been observed for carbon-doped silicon⁵ and for H⁻ and D⁻ impurities in the alkaline-earth fluorides.⁹

EXPERIMENTAL

The boron-doped silicon was grown with a B¹⁰ isotope (96.5% isotopic purity) or B¹¹ (98% isotopic purity). The samples were compensated by diffusion of lithium at 850°C using Li⁶ (99% isotopic purity) or with normal lithium (~92.5% Li⁷). The initial resistivities of the samples ranged from 0.0046 Ω cm to 0.00057 Ω cm corresponding to doping levels of about 2.5×10¹⁹ to 2×10²⁰ cm⁻³. The final resistivity ranged from about 1 Ω cm in the most heavily doped samples to >10³ Ω cm in the more lightly doped specimens.

The data were taken at room temperature (~22°C) on a double-beam spectrometer using a high-purity silicon specimen in the reference beam to obtain approximate cancellation of the residual lattice absorption in the region studied here, from $\nu = 700$ to 1400 cm⁻¹. Some distortion and a decrease in strength of the multiphonon bands, particularly in the region from 700

* Sponsored by the Technical Advisory Committee of the Joint Services Electronic Program.

¹ S. D. Smith and J. F. Angress, *Phys. Letters* **6**, 131 (1963).

² M. Waldner and W. G. Spitzer, *Bull. Am. Phys. Soc.* **10**, 368 (1965).

³ J. F. Angress, T. Arai, A. R. Goodwin, and S. D. Smith, in *Proceedings of the 7th International Conference on the Physics of Semiconductors* (Dunod Cie., Paris, 1964), p. 1115.

⁴ P. G. Dawber and R. J. Elliott, *Proc. Phys. Soc. (London)* **81**, 453 (1963).

⁵ R. C. Newman and J. B. Willis, *J. Phys. Chem. Solids* **26**, 373 (1965).

⁶ M. Balkanski and W. A. Nazarewicz, *J. Phys. Chem. Solids* **25**, 437 (1964).

⁷ W. G. Spitzer and M. Waldner, *J. Appl. Phys.* **36**, 2450 (1965); W. G. Spitzer and M. Waldner, *Phys. Rev. Letters* **14**, 223 (1965).

⁸ W. Hayes, *Phys. Rev.* **138**, A1227 (1965). This paper contains a discussion of the point-group symmetry associated with defects in a zinblende lattice.

⁹ W. Hayes, G. D. Jones, H. F. Macdonald, C. T. Sennett, and R. J. Elliott, *Proc. Roy. Soc. (London)* (to be published).

to 850 cm^{-1} , was found. The significant result however was that a number of absorption peaks or bands were found in the measurements of differential transmission, whose position depends upon the mass of the boron isotope and in some cases upon the mass of the lithium isotope. These peaks are thus not due to changes in multiphonon lattice-mode absorption, but rather represent an effect of the local lattice modes introduced by the boron and lithium impurities. A typical differential transmission curve is shown in Fig. 1 for a sample doped with B^{10} and normal Li. An approximate but smooth correction has been made for the attenuation caused by scattering and the residual free-carrier absorption in the sample. Because of the small absorption of some bands it was necessary to obtain the data at the wide effective slit width, $\Delta\nu \sim 10\text{ cm}^{-1}$. As a result of this (or because the bands are inherently broad) some overlapping structure may not be observed. All the bands of Fig. 1 are resolved with the exception of the broad peak at $\sim 1054\text{ cm}^{-1}$. When a combination of B^{11} and Li^6 is employed this particular peak splits into two overlapping but distinguishable bands with peaks at 1067 and 1033 cm^{-1} .

ASSIGNMENT OF ABSORPTION BANDS

The assignment of the various absorption bands involves frequency combinations of two types. First, there are those that are due to multiples or combinations of local mode frequencies, and second, those that fall outside this category. In the latter case, all but one of the observed frequencies may reasonably be assigned as combinations of local mode frequencies and frequencies corresponding to certain lattice phonons.

We list in Table I, for reference, the fundamental

TABLE I. Fundamental frequencies of the local mode for the various boron and lithium isotopic combinations.

	$\text{B}^{10}-\text{Li}^7$	$\text{B}^{11}-\text{Li}^7$	$\text{B}^{10}-\text{Li}^6$	$\text{B}^{11}-\text{Li}^6$
ν_1	681	655	683	657
ν_2	584	564	584	564
ν_3	644	620	644	620
ν_4	522	522	534	534

TABLE II. Observed location of peaks between ~ 800 to 1400 cm^{-1} for the various isotopic combinations. The calculated values are obtained from Table I.

Designation or assignment	Character	$\text{B}^{10}-\text{Li}^7$		$\text{B}^{11}-\text{Li}^7$		$\text{B}^{10}-\text{Li}^6$		$\text{B}^{11}-\text{Li}^6$	
		Expt	Calc	Expt	Calc	Expt	Calc	Expt	Calc
$2\nu_1$	Very weak	1354	1362	1304	1310	1355	1366	1312	1314
$2\nu_3$	Shoulder	1286	1288	1238	1240	1284	1288	1236	1240
$\nu_1+\nu_2$	Strong	1266	1265	1219	1219	1267	1267	1218	1221
ν_a	Weak	1198		1170		1200		1176	
$2\nu_2$	Strongest	1167	1168	1128	1128	1166	1168	1126	1128
ν_b	Very weak	1103		1081		
ν_c	Overlapping	1057		1031		1059		1033	
		1054		1037		1061			
$2\nu_4$		1044	1044	1044	1044	1067	1068	1067	1068
ν_d	Medium	964		943		961		944	
ν_e	Medium	916		888		917		885	

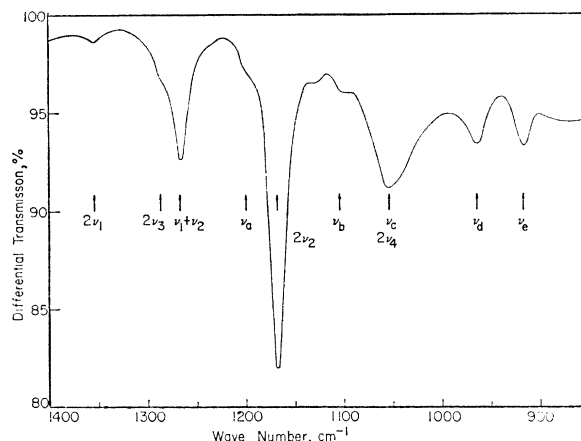


FIG. 1. Differential transmission of B^{10} and normal Li-doped silicon. Boron and lithium concentration $= 1.5 \times 10^{20}\text{ cm}^{-3}$. Sample thickness $= 8.5 \times 10^{-2}\text{ cm}$.

frequencies of the local modes for the various isotopic combinations.⁷ The ν_4 band is the lithium band, ν_3 is the boron band in the absence of paired lithium, ν_1 and ν_2 are the split-off bands due to B-Li pairs.

In Table II we list the location of all of the peaks which appear in the range 800 to 1400 cm^{-1} for the various isotopic combinations.

The determination of the frequencies of peak absorption is estimated to be reproducible to about $\pm 2\text{ cm}^{-1}$ in the case of the strongest peak and to $\pm 5\text{ cm}^{-1}$ in the case of the weakest features. In all cases except the $2\nu_4$ and ν_c bands only the boron substitution caused a measurable effect on the position of the bands. A few comments on the ν_c and $2\nu_4$ bands are necessary. Those values not in italics are the experimentally observed peak positions. Only in the $\text{B}^{11}-\text{Li}^6$ case was the $2\nu_4$ peak resolved from the ν_c peak (at 1033 cm^{-1}) which will be assigned later. Because of this observation it is believed that the observed peaks in the other 3 isotopic cases are the result of two unresolved overlapping bands. The values in italics are deduced on the basis of the $2\nu_4$ assignment and the ν_c assignment which will be made. The observed single feature in these cases falls between the deduced frequencies and would correspond

TABLE III. Assignment of bands involving silicon phonon frequencies.

Designation	Assignment	B ¹⁰ -Li ⁷			B ¹¹ -Li ⁷			B ¹⁰ -Li ⁶			B ¹¹ -Li ⁶		
		Expt	ν'	ν''	Expt	ν'	ν''	Expt	ν'	ν''	Expt	ν'	ν''
ν_a	$\nu_1 + \nu'$	1198	517		1170	515		1200	517		1176	519	
ν_b	$\nu_2 + \nu'$	1103	519		1081	517			
ν_c	$\nu_1 + \nu''$	1057		376	1031		376	1059		376	1033		376
ν_d	$\nu_2 + \nu''$	964		380	943		379	961		377	944		380

reasonably well with the values expected from the overlapping peaks. The very weak structure at ν_b (1103 or 1080 cm^{-1}) in the Li⁷ samples was not distinguishable in the Li⁶ samples. In this latter case the peaks would fall in a region where adjacent structure would mask them.

The assignments given in Table II are those due to the combination of local mode frequencies. Double frequencies of all the local modes plus the combination band $\nu_1 + \nu_2$ are observed, and the observed frequencies compared reasonably well with those calculated from Table I.

There is a question whether these bands are due to multiple quantum transitions at a single local mode site or perhaps due to interactions of near neighbor sites. A specimen containing 50% B¹⁰ and 50% B¹¹ was prepared and compensated with lithium. Except possibly in the cases where overlapping peaks occur, the absorption spectra was a superposition of the absorption found in B¹⁰- and B¹¹-doped silicon. In particular, the strongest peaks at $2\nu_2$ (1167 and 1128 cm^{-1}) and the strong peaks at $\nu_1 + \nu_2$ (1266 and 1219 cm^{-1}) appeared in equal strength. Peaks at the intermediate positions due to mixing of B¹⁰ and B¹¹ mode frequencies were not observed. Such bands would have been strong if there was an appreciable effect due to interactions of neighboring sites. Furthermore, over the range checked the strengths of the $2\nu_2$ and $\nu_1 + \nu_2$ bands were approximately proportional to the boron concentration.

The ratio of peak absorption coefficient to impurity concentration is $\sim 1.1 \times 10^{-20} \text{ cm}^2$ for the $2\nu_2$ band and $\sim 0.5 \times 10^{-20} \text{ cm}^2$ for the $\nu_2 + \nu_1$ band. The strength of the ν_2 fundamental is ~ 90 times that of the $2\nu_2$ overtone. Finally, it may be noted that, with the possible exception of the 1103, 1081 cm^{-1} pair, no bands are observed which can be explained as $\nu_1 + \nu_4$ or $\nu_2 + \nu_4$. With the assumption of the weak boron-lithium force constant, to explain the small lithium isotope shift of the ν_1 and ν_2 fundamental bands, this result is not surprising. Combinations of frequencies associated with different centers are not observed.

It is of interest to note that the absorption strengths of the multiple transitions associated with the boron local modes are in the order $\alpha(2\nu_2) > \alpha(\nu_1 + \nu_2) > \alpha(2\nu_1)$, while for the fundamental absorption $\alpha(\nu_2) < \alpha(\nu_1)$. This indicates that the anharmonicity of the ν_2 mode is substantially greater than that of the ν_1 mode. The $2\nu_3$ absorption is relatively weak shoulder; however, it has

also been observed as an isolated band in boron-doped silicon largely compensated during growth with antimony. Lithium was used then only to complete the compensation.

There are five bands remaining in Table II which cannot be explained in terms of combinations of two local-mode frequencies. Comparison of Table II with Table I shows that the shifts between B¹⁰ and B¹¹ of $\nu = 20$ to 28 cm^{-1} correspond to the participation of only one local mode. Moreover $\nu_a - \nu_b \approx \nu_c - \nu_d \approx \nu_1 - \nu_2$ for both B¹⁰ and B¹¹. This suggests the further assignments of Table III. The values of ν' and ν'' determined from the experimental results are in reasonable agreement with certain unperturbed silicon phonon energies.¹⁰ The ν' is close to 518 cm^{-1} , the optical modes at the zone center (Γ point). The ν'' is near 371 cm^{-1} , the longitudinal modes at the zone edge in the $[1\frac{1}{2}0]$ direction (W point) and near 377 cm^{-1} , the longitudinal-acoustic phonon at the zone edge in the $[111]$ direction (L point).

The remaining band, ν_e of Table II, is not compatible with the combination of any local mode of Table I, dependent on boron isotope, with any silicon critical-point phonon frequency. While the frequencies are close to some recently reported oxygen bands in silicon,¹¹ the boron isotope effect rules out such an identification. In fact, comparison with low-oxygen-content silicon indicates all of the oxygen bands were absent in these lithium-diffused samples with the possible exception of a very weak absorption near 1010 cm^{-1} , due to a Si-Li-O absorption band.¹² Therefore, at the present time, the source of the ν_e band is uncertain.

DISCUSSION

It has been pointed out⁸ that in the rigid-lattice approximation, the potential of a substitutional impurity in a silicon lattice to the fourth order in impurity displacement is

$$V = V_0 + A(x^2 + y^2 + z^2) + B(xyz) + C_1(x^4 + y^4 + z^4) + C_2(x^2y^2 + y^2z^2 + x^2z^2). \quad (1)$$

¹⁰ F. A. Johnson, Progr. Semicond. (to be published); R. Loudon and F. A. Johnson, in *Proceedings of the 7th International Conference on the Physics of Semiconductors* (Dunod Cie., Paris, 1964), p. 1037.

¹¹ J. W. Corbett, G. D. Watkins, and R. S. McDonald, Phys. Rev. **135**, A1381 (1964).

¹² E. M. Pell, in *Solid State Physics in Electronics and Telecommunications*, edited by M. Desirant and J. L. Michiels (Academic Press Inc., New York, 1960), Vol. I, Part I.

Because of the presence of anharmonic terms in the potential, overtones of the fundamental vibration are no longer forbidden and we are able to observe bands near twice the unpaired boron mode frequencies, i.e., $2\nu_3$. The weakness of these bands indicates that the coefficients of the anharmonic terms are small.

When an interstitial lithium ion pairs with the substitutional boron impurity, we can anticipate that the tetrahedral point-group symmetry at the boron site is at least lowered to one with axial symmetry where the threefold-degenerate optically active boron mode is split by the presence of the lithium into a single and doubly degenerate mode⁸ with a strength ratio of 1 to 2. This appears to be the case in the present work¹³ and was also recently reported for substitutional Li-compensated Te-doped GaAs⁸ where the modes are attributed to a Li-Te pair.

A simple model may be given which qualitatively appears to explain many of the experimental results for the B-Li pair bands and some of the characteristics of the overtone bands. For the purposes of the present explanation, we will use the harmonic approximation for V at the boron site before Li pairing, i.e., $B=C_1=C_2=0$ and $V=V_0+Ar^2$. After pairing V becomes

$$V = V_0 + Ar^2 - q^2/\epsilon'\xi + R/\xi^n, \quad (2)$$

where ξ is the B-Li bond distance, ϵ' is the effective dielectric constant for a dipole of spacing ξ , and the last term is the B-Li repulsive potential. We have neglected any distortion of the B-Si tetrahedron because of Li-Si interactions. For axial displacement, the force is given by

$$f_r = -2Ar + (q^2/\epsilon'\xi^2 - nR/\xi^{n+1}). \quad (3)$$

If the equilibrium pair spacing is determined only by the B-Li interaction the term

$$q^2/\epsilon'\xi^2 - nR/\xi^{n+1} = 0, \quad (4)$$

and the effective force constant for the boron is given by

$$k = 2A - (2q^2/\epsilon'\xi_0^3)[1 - (n+1)/2], \quad (5)$$

where ξ_0 is the equilibrium pair spacing. For most ionic crystals¹⁴ $6 \leq n \leq 12$ and hence the force constant for unpaired boron k_0 would be increased for the non-degenerate axial mode. This is opposite the observed splitting where the triply degenerate boron mode is split by Li pairing into two bands with strengths in the ratio of ~ 2 to 1, but where the weaker one is the low-frequency mode. This discrepancy is eliminated if (4) is not the relation establishing $\xi = \xi_0$ and the B-Li repulsive force is small. In this case,

$$k \sim k_0 - 2q^2/\epsilon'\xi_0^3 \quad (6)$$

for the axial mode, and

$$k \sim k_0 + q^2/\epsilon'\xi_0^3 \quad (7)$$

for the doubly degenerate mode. The shifts are then in the correct direction and using the measured shift of the low-frequency mode we obtain $\xi_0 = 2.1 \text{ \AA}/(\epsilon')^{1/3}$. Comparison with previously estimated values for ξ_0 , of 2.2 to 2.4 \AA , indicates ϵ' should be close to 1. Note that ϵ' is the local effective dielectric constant rather than an average value near 12 used to calculate ξ_0 from the pair dissociation energy.¹⁵ Moreover $\Delta k \sim q^2/\epsilon'\xi_0^3 \sim 0.1 k_0$, which is reasonable in view of the lack of dependence of the 681- and 585-cm⁻¹ mode frequencies on Li isotope. In this weak-coupling case, very little of the energy of these modes would be in Li motion.

If the anharmonic terms in the electrostatic part of (2) are included, then one finds that the axial force includes terms of all positive powers of the displacement while the force orthogonal to ξ has only terms involving odd powers of the displacement. Therefore, it is to be anticipated that the overtone of the axial mode would be much stronger than that for the doubly degenerate modes. This is in agreement with observation $\alpha(2\nu_2) > \alpha(\nu_1 + \nu_2) > \alpha(2\nu_1)$. The anharmonicity of the force constant, assuming that ϵ' is independent of displacement, is however insufficient to account for the strength of the overtone bands.¹⁶ The appearance of absorption bands which involve the sums of local mode and lattice frequencies may be due to terms which have been omitted from (1) and arise when the rigid lattice approximation is relaxed. The second-order electric-moment term may also be of importance. These terms which couple the local and lattice modes are also responsible⁹ for contributions to the local mode absorption bands linewidth and temperature dependence of the peak position. It is also to be expected that these local-lattice combination modes will be dependent on the phonon density of states. It is therefore significant that the phonon energies involved are close to values at definite critical points rather than peaks in the average single phonon density-of-states curve.¹⁰

The assumption that the Li-B repulsion is not primarily responsible for establishing the equilibrium pair spacing is in agreement with the following observation. For Al-Li, Ga-Li, and In-Li pairing in Ge, the calculated pair spacings are in reasonable agreement with the sum of the acceptor covalent and Li ionic radii while B-Li pairs in both Ge and Si have spacings substantially larger than the sum of the radii.¹⁵ Therefore, it is not surprising that the Li-B repulsive term is small. The interaction which establishes the equilibrium ξ may have a contribution from the interaction between

¹³ From Ref. 7 the actual ratio may be closer to 3 to 5.

¹⁴ See, for example, A. J. Dekker, in *Solid State Physics* (Prentice-Hall, Inc., Englewood Cliffs, New Jersey, 1957), p. 122.

¹⁵ F. A. Kroger, *Chemistry of Imperfect Crystals* (North-Holland Publishing Company, Amsterdam, 1964), p. 272.

¹⁶ J. L. Dunham, *Phys. Rev.* **35**, 1347 (1930).

the Li⁺ and the Si atoms.^{17,18} The model employed here is very much simplified; however, it does appear to explain, in a qualitative fashion, many of the observed features.

SUMMARY

New absorption bands are observed in boron-lithium-doped silicon. Some of these bands are due to double-quantum transitions in local modes at individual

impurity sites. The relative strengths of the absorption show the greatest anharmonicity in the vibration of the lowest frequency local mode produced by the boron-lithium impurities. Four of the five remaining bands may be ascribed to combinations of the two strongest local modes with silicon critical-point phonon frequencies.

ACKNOWLEDGMENTS

The authors wish to thank M. H. L. Pryce, H. Reiss, J. Smit, F. A. Kroger, and D. Dows for helpful discussions and P. E. McQuaid for the preparations of the specimens.

¹⁷ J. S. Prener and F. E. Williams, *J. Chem. Phys.* **35**, 1803 (1961).

¹⁸ K. Weiser, *Phys. Rev.* **120**, 1427 (1962).

Defect Structure of Crystalline Quartz. II. Variation of Displacement Threshold Energy with Crystal Growth Rate*

GEORGE W. ARNOLD

Sandia Laboratory, Albuquerque, New Mexico

(Received 30 April 1965)

An optical-absorption maximum (*C* band) is produced at about 220 $m\mu$ in crystalline quartz by electron bombardment at 77°K. The band is produced by the displacement of lattice atoms and not by ionization. Previously it was shown that the production rate of the band for constant integrated electron flux increases greatly with increased growth rate. In the present experiment, the threshold energy for the displacement which leads to *C*-band absorption was measured in synthetic crystalline quartz grown at 0.45 and 1.91 mm/day. Interpretations of the data lead to the conclusion that *C*-band absorption is caused by displacement of oxygen atoms and that the threshold energy for this displacement is a function of growth rate varying from 15 ± 5 eV for fast-growth (1.91 mm/day) material to 50 ± 5 eV for quartz grown at a slower rate (0.45 mm/day).

I. INTRODUCTION

CRYSTALLINE quartz develops an absorption band (*C* band) in the near ultraviolet when bombarded with fast electrons or neutrons. For electron bombardment, this band lies near 220 $m\mu$. Its characteristics have been discussed in an earlier paper.¹ It was shown there that, for constant time-integrated electron flux, the production rate of the defects responsible for the *C*-band absorption in synthetic quartz increased by a factor of 17 as the growth rate increased by a factor of 4.5. Since the *C*-band absorption was shown to be due to a displacement process, this defect-production-rate variation with crystal growth rate suggests that the threshold displacement energy may also vary with rate of growth. The present paper reports measurements of the threshold displacement energy in synthetic crystalline quartz and its variation with crystal growth rate using the optical absorption of the *C* band produced by electron irradiation.

II. BACKGROUND

The threshold energy E_d , for displacement of a lattice atom is that energy which, when transmitted to the atom, will just dislodge it from its site. The assumptions made in the Seitz-Koehler² formalism in defining the cross section for displacement by relativistic electrons are used. In this paper a step function is assumed for the threshold energy, i.e., no atoms will be dislodged for an electron energy below E_t , which transmits a maximum energy of E_d , and all atoms given an energy of E_d or greater will be displaced with unit probability.

The number of displaced atoms per cm^3 produced by electron bombardment for energies greater than that required for displacement is given by $N_d = N_0 \sigma_d \Phi \bar{\nu}$, where N_0 is the number of target atoms/ cm^3 , σ_d is the cross section for primary atom displacement in cm^2 , Φ is the electron flux in e/cm^2 , and $\bar{\nu}$ is the number of secondary target-atom displacements per primary displacement. The displacement cross section σ_d is a

* This work was supported by the U. S. Atomic Energy Commission.

¹ G. W. Arnold, *Phys. Rev.* **139**, A1234 (1965).

² F. Seitz and J. S. Koehler, *Solid State Physics* (Academic Press Inc., New York, 1956), Vol. 2, p. 305.